Effect of Low Frequency Thermal Cycling on the Crack Susceptibility of Soldered Joints

Mechanism of cracking in four solder alloys used on PCB joints is studied during and after cycling from −65 to + 150 C

BY E. R. BANGS AND R. E. BEAL

ABSTRACT. Increasing interest has been directed toward the problem of solder joint cracking in printed circuit boards. Previous investigations have dealt with the effect of high frequency thermal cycling on the cracking of soldered joints and the effect of gold plated leads on susceptibility. The present program involved the effect on joints when exposed to low frequency thermal cycling and a definition of the metallurgical cracking mechanism.

Four solder alloys (50Sn-50Pb, 63Sn-37Pb, 70Sn-30Pb, and 40Sn-60Pb) were exposed to low frequency thermal cycles. Sample soldered joints on printed circuit boards were installed in an environmental test chamber and subjected to thermal cycling which consisted of holding the boards at −65 C for 30 min, immediately exposing the boards to +150 C, and holding at that temperature for 30 min. The PCBs were then cycled until a failure was indicated by the monitoring system or 800 cycles was reached. Although actual solder joint failure occurred only with the 63Sn-37Pb alloy, varying degrees of cracking existed in all of the boards tested after 800 cycles.

An exhaustive study was performed on the tested soldered joints to detect any metallurgical changes resulting from testing and to define the metallurgical mechanism of solder failure. Examinations consisted of bright-light microscopy and scanning electron microscopy on soldered fillet faces, joint cross-sections, and fractured surfaces.

It has been clearly demonstrated that soldered joints crack rapidly when exposed to low frequency thermal cycling. In addition, due to appreciable changes in the microstructure morphology as a result of cyclic testing, it is possible to define the mechanism of cracking in the soldered joint.

E. R. BANGS is associated with and R. E. BEAL is Assistant Director of the Metals Research group of the IIT Research Institute, Chicago, Illinois 60616.

Paper was presented at the 4th International Soldering Conference held during the 56th AWS Annual Meeting in Cleveland, Ohio, April 21-25, 1975.

Introduction

During recent years the problems associated with cracking of solder joints, particularly where thermal cycling is involved, have generated increased interest. Previous investigations on the subject have resulted in

Table 1 — Solder Alloy Compositions, wt %[a]

Alloy	Sn	Sb	Bi	Cu[b]	Fe[b]	Zn[b]	Al[b]	As[b]	Approx. melting range, F deg Solidus	Liquidus
Sn70	69.5-71.5	0.20-0.50	0.25	0.08	0.02	0.005	0.005	0.03	360	380
Sn63	62.5-63.5	0.20-0.50	0.25	0.08	0.02	0.005	0.005	0.03	360	360
Sn50	49.5-51.5	0.20-0.50	0.25	0.08	0.02	0.005	0.005	0.025	360	420
Sn40	39.5-41.5	0.20-0.50	0.25	0.08	0.02	0.005	0.005	0.02	360	460

(a) Total of all other elements 0.08 wt% maximum; balance Pb.
(b) Maximum.

general conflicting conclusions as to the basic cause of cracking in joints. A definition of the metallurgical cracking mechanism has received superficial treatment and remained questionable. Problem incidence has been considerably reduced by attention to component lead designs, hole dimensions, properties of surfaces, and intermetallic compound formation, but a full understanding still eludes investigators.

The present program has approached the problem by selecting four solder alloys (70Sn-30Pb, 63Sn-37Pb, 50Sn-50Pb, 40Sn-60Pb) and producing a controlled series of printed circuit boards (PCB) for evaluation by thermal cycling. The four solders chosen represent materials with both primary lead- and primary tin-rich dendrites in a lead-tin eutectic matrix to effectively cover the entire tin-lead system. Commercially produced polyimide boards with plated through-holes and multiple dual in-line integrated circuit pads have been used. One series of boards was tin-lead plated; a second series was soldered coated in accordance with MIL-M-38510.

For thermal cycling, a test criterion of failure was 10% of soldered connections being tested or 800 h test duration — whichever occurred first. The test program included electrical monitoring, visual examination, metallography by bright light, and scanning electron microscopy. Solder joints exposed to low frequency thermal cycling clearly are susceptible to joint cracking. The eutectic alloy, 63Sn alloy, cracked most severely and gave poorest life test results. A mechanism of solder alloy cracking was positively established.

PCB Preparation

Materials

Commercial printed circuit boards 1/16 in. thick made from a polyimide material were used in the program. The solder joint test work involved a series of 12 dual in-line integrated circuit module pads on each board with dummy integrated circuit modules, using the pins only as a test medium for circuit continuity. Tin-plated Kovar leads were used on the integrated circuit packages.

The solder alloys were Sn70, Sn63, Sn50, and Sn40 as shown in Table 1, with residual elemental anaylses shown in Table 2. The boards with each solder alloy were plated, and two were reflowed and two tested in the as-received condition.

PCB Modification

To facilitate obtaining and using suitable PCBs for the program, an existing design polyimide board was purchased. The board had twelve dual in-line integrated circuit assemblies within a 4-1/4 × 3-1/8 × 1/16 in. area. The circuits were modified to enable making 94 connections for test program purposes.

Circuit Continuity Design

After careful consideration of all possible alternates, it was determined most practicable to use a light-emitting diode (LED) system of circuit continuity monitoring. A con-

Table 2 — Elemental Analysis of Four Solder Alloys, wt %

Element	Alloys having nominal tin-lead contents of: 70-30	63-37	50-50	40-60
Tin	70.47[a]	63.14	50.25	40.61
Lead	29.15	36.52	49.18	59.02
Antimony		0.28	0.34	0.28
Bismuth		<0.005	<0.005	<0.005
Copper		<0.005	0.012	<0.005
Iron		<0.005	<0.005	<0.005
Zinc		<0.005	<0.005	<0.005
Aluminum		<0.005	0.07	<0.005
Phosphorus		0.001	0.001	0.001
Sulfur		0.010	0.014	0.008
Arsenic		0.01	0.03	<0.01
Gold		<0.01	<0.01	<0.01
Magnesium		<0.005	<0.005	<0.005
Nickel		<0.005	<0.005	<0.005
Silver		<0.005	<0.005	<0.005
Cadmium		<0.005	<0.005	<0.005

(a) Pure Sn was added to the 40-60 alloy to achieve this analysis.

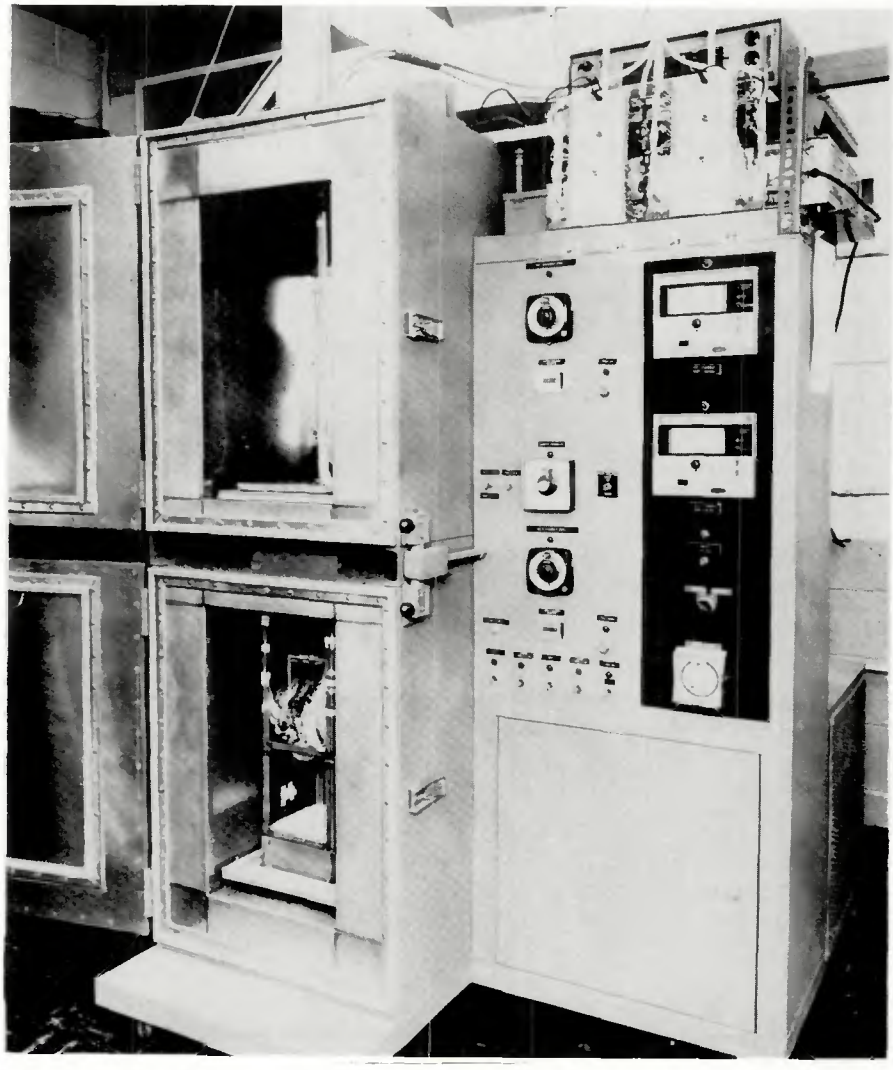

Fig. 1 — Environmental test chamber including monitoring and control system

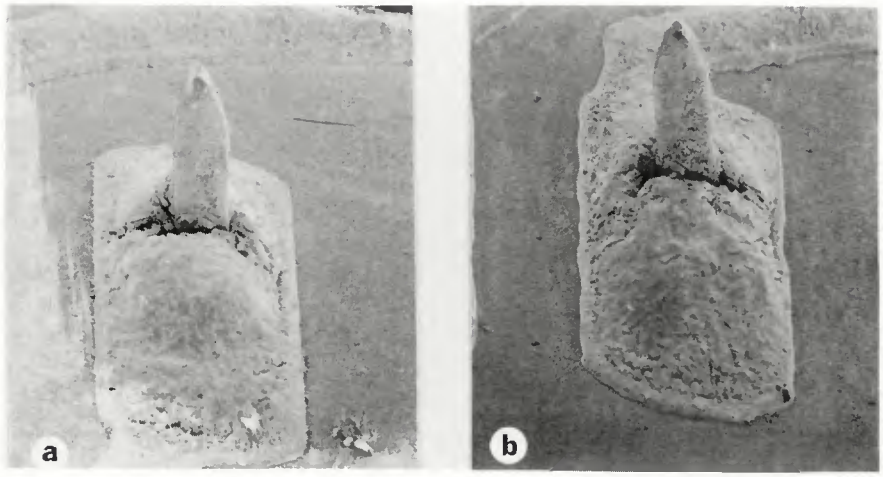

Fig. 2 — SEM view of PCB solder joints containing 63Sn alloy after environmental testing. (a) Integrated circuit pin on reflow soldered PCB; (b) same on nonreflow soldered PCB X25, reduced 39%

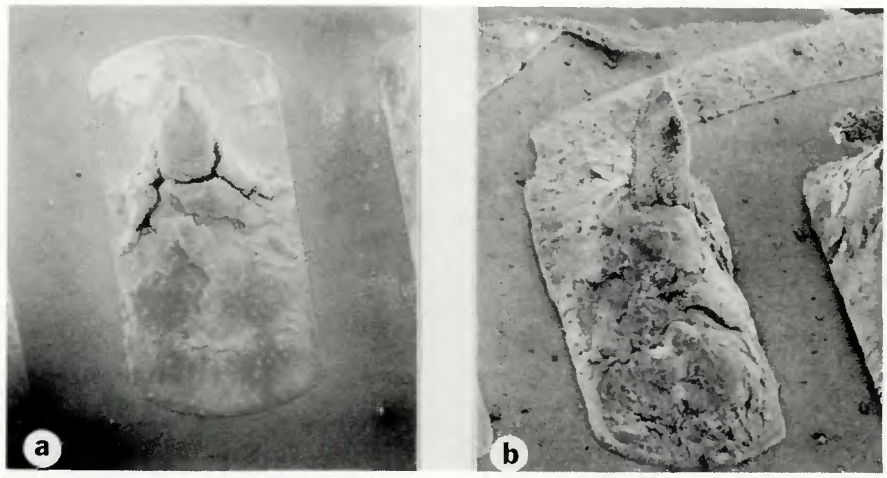

Fig. 3 — SEM view of PCB solder joints with 50Sn alloy after environmental testing. (a) Integrated circuit pin on reflow soldered PCB; (b) same on plated soldered PCB. X25, reduced 38%

stant power supply was connected through a common limiting resistor to the LEDs. Each diode was connected to an individual solder joint on the test board and back to the power supply, Fig. 1, top right.

Two main considerations in overall test circuit design were the large number of wires and the need for a low current device so that fine gage wires could be assembled in an umbilical cord to be fed through the wall of the thermal shock chamber. Each cable consisted of 94 No. 40 and 2 No. 16 stranded Teflon insulated wires inside Teflon tubing with both ends of each wire identified by a marker, connected at the monitoring end of the system.

The Teflon-sleeved wire bundles were fed through the top of the thermal shock chamber with enough extension to accommodate the movements from cold to hot chamber. Because of circuit resistance requirements, it was impossible to provide a plug-in type connector set. The resistance across such a connection would have been higher than the resistance across the joints to be monitored. Consequently, individual wires had to be soldered to the integrated circuit pins to provide the circuit continuity. All circuits were then carefully checked for continuity and uniform resistance before placing the boards in the test rack. Four main cables were connected to eight PCBs for a test run. Only four boards could be monitored at one time, however, so a switching arrangement was included in the circuit to provide necessary monitoring control.

The test rack assembly with eight boards ready for test is seen in Fig. 1. The main cables extend from the lower chamber (cold zone) through the upper chamber (hot zone) outside through the top opening to the monitoring system.

Figure 1 also shows the equipment and materials all ready for a test run. For monitoring purposes, the

Fig. 4 — As-soldered plated integrated circuit joint soldered with 63Sn alloy. X170, reduced 37%

resistance necessary at a soldered joint to turn off the light-emitting diode was established. A reference voltage that required only 500 ohm charge to turn out the light was selected and used throughout, measured at 1.510 volts. To ensure consistency within the testing program, a documented procedure for assembly, monitoring, and removal of specimens was prepared and maintained for reference.

Thermal Cycle Testing

Test Details

A thermal test cycle consisted of exposure at −65 C for 30 min followed by +150 C for 30 min with a 3 min interval to allow transfer between chambers and attain the appropriate chamber temperature. Continuous monitoring as previously described was performed with 94 joints on each board under observation. The criterion used during the program was failure of 10% of the soldered connections.

Circuit Continuity Observations

The first test run with 63Sn and 50Sn alloys was concluded at 800 cycles. The reflowed printed circuit board soldered with the 63Sn alloy contained the highest incidence of solder joint cracking. Examination of the soldered joints revealed failures comprised of large open cracks in the solder fillets and areas in which particles of the solder alloy actually broke away, as shown in Figs. 2 and 3.

Based upon the LED indications, 15 soldered joints had failed on the 63/37 reflow soldered board. There were no other LED indicator failures on the other boards tested. Resistance measurements were per-

formed on the 15 failed solder joints by a four-terminal Kelvin technique to determine where in the circuit the increased resistance had occurred. In 12 of the 15 joints, the resistance between the integrated circuit pin and the printed circuit board had increased sufficiently to extinguish the indicator lights. In the remaining three joints, the resistance increase apparently occurred in the lead wire attachment, the jumper connections on the PCB, or other PCB printed circuitry.

Thermal cycle testing performed on the 70Sn and the 40Sn alloys resulted in a completion of 800 cycles without evidence of a failure by extinguishing of an LED. The soldered joints were representative of printed circuit boards in the solder plated condition and the solder coated or reflowed condition. However, it should be noted that after voltage measurements were taken on the tested circuits, resistance had increased.

Surface Cracking Identification

Surface cracking was evident on all the soldered connections contained in the printed circuit boards. Cracks were located at both the pin side of the soldered joints and the component (integrated circuit) side of all the soldered joints tested. The overall crack locations were similar on joints soldered with the 70Sn, 63Sn, 50Sn, and 40Sn alloys. In all cases cracking was initiated at the solder-fillet toe region adjacent to the integrated circuit pin. In all cases the crack existed for 360 deg around the lead. Those joints soldered with 70Sn and 63Sn alloy contained a more severe amount of cracking with larger, deeper cracks. In addition to extensive cracking, fragments of solder were removed from the face regions of the fillet.

Metallurgical Examination

63Sn-37Pb Soldered Joints

Figure 4 shows a section of the 63Sn alloy plated integrated circuit soldered joint in the as-soldered condition containing the fine eutectic microstructure. Figure 5 shows a fillet after exposure to 800 cycles without failure of LEDs. Cracking is evident near the pin lead and the upper tapered region; the cracking follows the pin in a very linear manner. Fractured regions of the solder alloy fillet toe at the pin interface showed evidence of solder alloy loss and deformation during thermal cycling. The solder alloy microstructure adjacent to the pin in the fillet throat region and near the copper-plated board has coarsened. The type of cracking that will be defined here as thermal fatigue cracks shows characteristics of both a failure due to stress rupture and fatigue, as revealed in the copper-clad region of the PCB in which a linear fracture follows the surface of the solder plated zone.

With the 63Sn solder alloy on a reflowed printed circuit board, approximately 10% of the light-emitting diodes under surveillance extinguished at 800 cycles of environmental testing.

An examination of the fractured surfaces using the SEM revealed further data relating to the fracture mechanism of the joints with 63-37 solder alloys. Figure 6 is representative of the fractured 63-37 solder alloy interface on the pin side of the soldered joint. The fracture had a nonductile fracture appearance in areas of coarsened eutectic distribution combined with interphase separation. Plastic deformation has occurred during crack propagation. Fracture due to slip is occurring combined with evidence of twinning lamellae in the tin-lead matrix.

50Sn-50Pb Soldered Joints

Figures 7 and 8 are representative of the 50Sn-50Pb joints on plated and reflowed solder alloy PCBs. The characteristics of the cracks of the reflowed and plated joints were similar. Cracks were evident propagating from the solder fillet toe at the pin region. There was no extinguishing of light-emitting diodes upon completion of cycling at 800 cycles. The cracks follow the pin interface with the presence of grain coarsening adjacent to the crack opening. Areas in the toe region of the fillet contained fragmented solder material.

The fracture interface of the 50-50

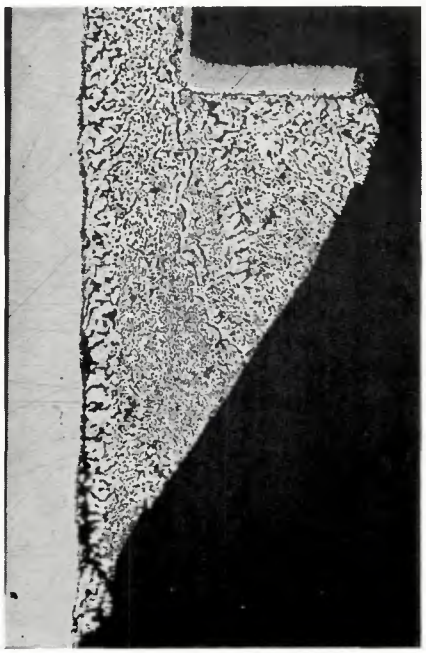

Fig. 5 — Stress-rupture and thermal fatigue failures in pin region of 63Sn solder alloy on plated soldered PCB. X170, reduced 50%

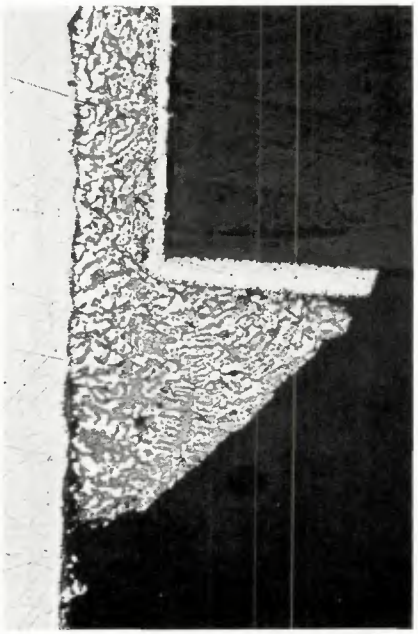

Fig. 7 — Integrated circuit joint (pin side) containing 50Sn-50Pb solder alloy on plated soldered PCB. x170, reduced 50%

Fig. 6 — SEM view of 63Sn-37Pb solder alloy fractured interface between pin and fillet face of reflowed board. X3000, reduced 48%

Fig. 8 — SEM view of 50Sn-50Pb solder alloy on reflowed PCB, intersection of crack on solder fillet face. X750, reduced 47%

solder alloy revealed a grain structure morphology of nonductile fine fractures in the solder alloy layer remaining on the pin surface. Fractures along the coarsened twinned lamellae were prevalent in the solder alloy tin-lead matrix. The fractured surfaces of the 50-50 alloy were much coarser than the eutectic alloy. However, the depth of cracking was less than the eutectic alloy and more ductile.

The fracture and deformation characteristics of the reflowed PCB were similar to the plated PCB. Figure 7 shows intergranular disintegration on the solder alloy fillet face. Figure 8 shows the intersecting area of the crack that proceeds to open and surround the pin. Crack propagation is occurring in an intergranular manner.

There were no major differences in the defect characteristics of the reflowed and plated boards soldered with the 50-50 solder alloy. The surface cracking condition was much finer in appearance than the eutectic solder with some open cracking more prevalent adjacent to the component lead and solder alloy.

40Sn-60Pb Soldered Joints

Figure 9(a) shows the 40Sn plated soldered joint prior to thermal cycling. The microstructure contains the lead-rich matrix with sharply defined eutectic and dendritic branches. Figure 9(b) shows the soldered fillet after exposure to 800 cycles of thermal testing with a drastically transformed microstructure after being subjected to thermal and mechanical stressing.

After exposure to 800 thermal cycles, crack initiation occurred at the solder fillet toe adjacent to the lead pin. Extensive grain coarsening was produced, with excessive amounts of lead-rich phase present in the crack area at the solder/pin interface.

Extensive fragmentation occurred primarily in the fractured interface at the crack initiation zone.

70Sn-30Pb Soldered Joints

The nature of the cracking that occurred in the 70Sn alloy confirmed the magnitude of the shear stress imposed on the solder/pin interface during pin growth on heatup. Gross cracking and separation between the solder fillet and pin was evident. Considerable tin-rich grain coarsening occurred in the highly stressed pin leg and throat regions of the fillet. Cracks propagated perpendicular to the pin surface through the lead-rich phases and across tin-rich grains.

Figure 10(a) shows the tin-rich microstructure of the 70Sn soldered joint of the reflowed PCB prior to testing. Figure 10(b) shows the fillet after 800 cycles of thermal testing. As can be observed, the microstructure has undergone a drastic transformation to a coarsened eutectic distribution in which cracking has occurred through areas of excessive coarsening.

Figure 11 shows the gross cracking condition which exists at the pin fillet leg region and multi-directional cracking existing in the throat region of the fillet. The cracking condition describes clearly the "hinge" effect created through the throat region of the fillet. As shown at A the crack path has propagated transverse to the throat direction of the fillet. Hairline cracking can be detected through the lead-rich layers extending perpendicular to the pin/fillet crack interface. As shown in B, hairline crack

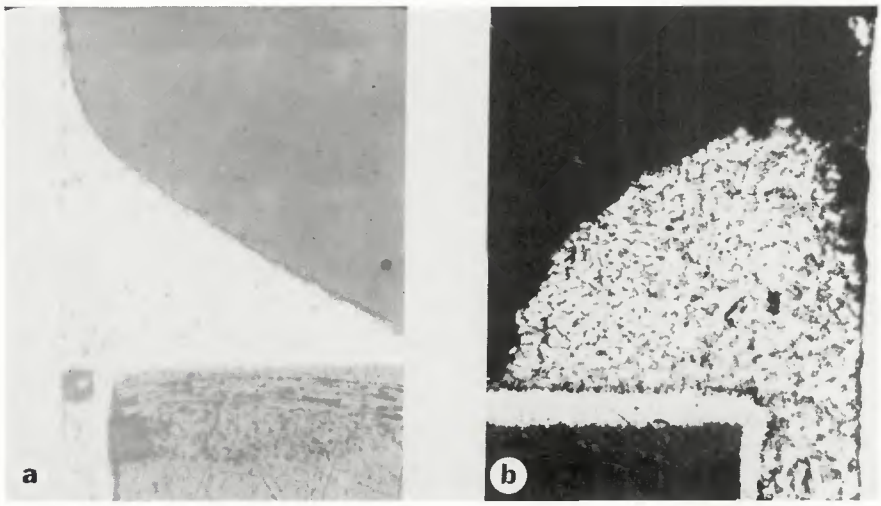

Fig. 9 -- Thermally cycled 40Sn-60Pb soldered plated joint (a) in the as-soldered condition and (b) after exposure to 800 cycles of environmental testing. X170, reduced 40%

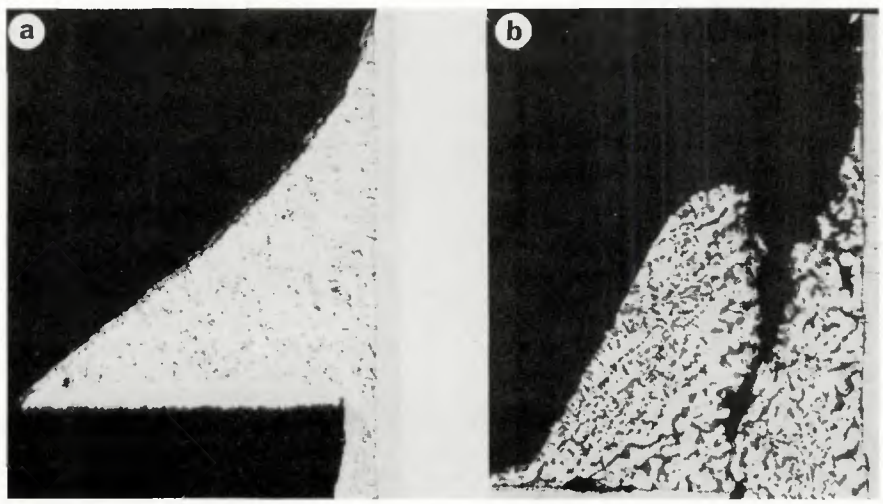

Fig. 10 — Thermally cycled 70Sn alloy soldered joint (a) in the as-soldered condition and (b) after exposure to 800 cycles. X170, reduced 40%

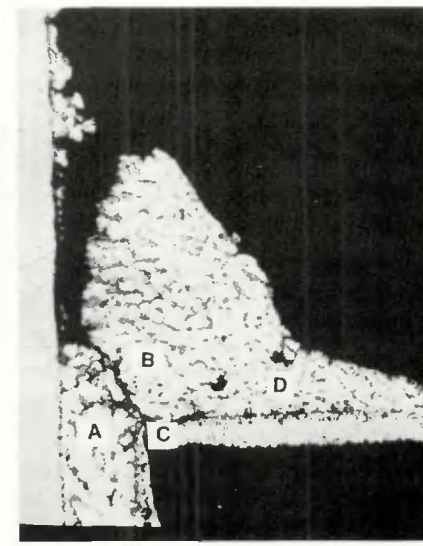

Fig. 11 — Plated soldered joint with 70Sn-30Pb alloy after exposure to 800 cycles of thermal cycling containing multidirectional microstructural cracking and fragmentation of solder alloy. X170, reduced 37%

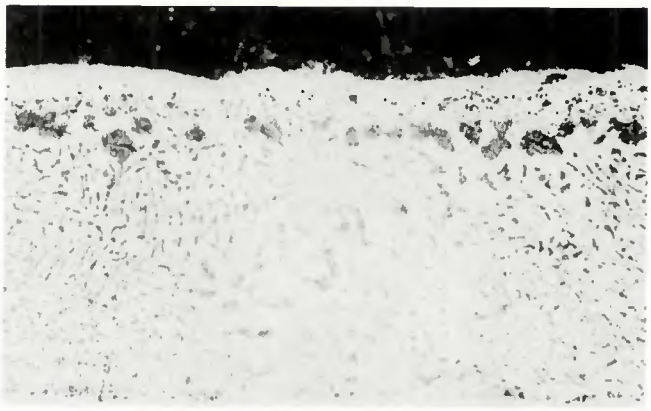

Fig. 12 — Growth of lead-rich phase in 63Sn reflowed PCB at solder/copper clad interface. X480, reduced 49%

Fig. 13 — Crack along pin interface, mainly intergranular in form; 63Sn alloy. X480, reduced 49%

growth is occurring through the tin-rich grains. Crack formation is starting between points C and D which is an early stage of fillet fragmentation.

Discussion

Crack initiation usually is within the bulk solder alloy at the position of highest stress within the joint. Cracks propagate toward the interface and then travel at or adjacent to this region as shown in the 63Sn alloy soldered joint (Fig. 5) after testing. Crack initiation, therefore, is generally dependent upon solder alloy composition, joint area design, and the interface conditions. Crack propagation is strongly influenced by morphological conditions adjacent to and within the interface zone. However, observations also have demonstrated that where sufficient stress concentration exists, thermal cycling of a soldered joint can result in the generation of internal cracks within the solder at the interface in the zone of stress concentration. Under these circumstances, the interface qualities alone will dictate the life of the particular joint with cracks extending outwards from this zone of high stress concentration.

Incipient crack formation at the fillet leg interface of the PCB copper cladding due to the variation in thermal coefficient between the solder alloy, copper clad, and polyimide board material was observed. The solder alloy was 50Sn compositon on a plated PCB and the board had been subjected to 800 cycles of testing.

A major difference in the microstructure of the reflowed joint compared to the plated joint is the spheroidal phase evident in the reflow region of the PCB, Fig. 12. A similar spheroidal phase is shown in some regions at the solder alloy/pin interface. The reflowed layer is thicker than the plated layer. The solder in this area, because of added soldering temperature exposure, has diffused further into the copper cladding, thus changing the characteristic of the diffused interface between the reflowed layer and the plated structures.

The rate of intermetallic compound growth at the interface initially depends upon the tin content of the solder alloy and the solder process parameters when soldering the joint. Once the tin is substantially depleted from this area, a lead-rich layer is formed. Diffusion rates now are controlled by the thickness of the intermetallic zone and the resulting thickness of the lead-rich layer. Since thicknesses of both these layers can have a profound influence on the cracking mechanism of the joint within this region, a full knowledge of previous thermal history is important to an understanding of morphological change and the possibilities of crack formation and growth.

Mechanical properties also are influenced by these reactions, because it is known that peel strengths are reduced with increasing thicknesses of the intermetallic region. As the lead-rich layer grows, it is also conceivable that the rupture or fatigue strength of the zone will change since effectively composition is locally very different from the starting material. Again, unless careful characterization of these interfaces and their histories is performed, it will be possible to have apparently anomalous behavior.

The stress applied to the soldered fillet is caused by variations in the thermal coefficients of expansion between the solder alloy, the pin lead, the copper PCB cladding, and the polyimide board material. Their coefficients of expansion ae shown in Table 3.

In addition, diffusion rates can be strain accelerated as well as thermally affected.

Interface cracking was typically intergranular along the interface between tin-rich and lead-rich regions.

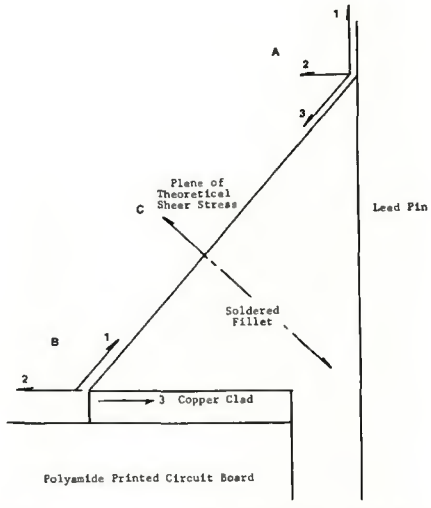

Fig. 14 — Model of stresses applied to the soldered printed circuit board joint during thermal cycling

Table 3 — Linear Thermal Expansion Coefficients

Material	Temp., C	Coef. of expan., μ in./in./C
Copper	20	16.5
Solder		
63Sn alloy	15-110	24.7
70Sn alloy	15-110	21.6
Polyimide PCB		
Z-direction	25-150	55
X-Y-dir.	25-150	35
Kovar (IC lead material)	—	5.5

Occasionally, cracking is through lead-rich regions or between tin-rich grains as shown in Figs. 35 and 36.

The model in Fig. 14 diagramatically shows the stresses applied to the fillet when the joint is subjected to 150 C. The stress concentration regions are the fillet toes at the pin A and the copper cladding B. During

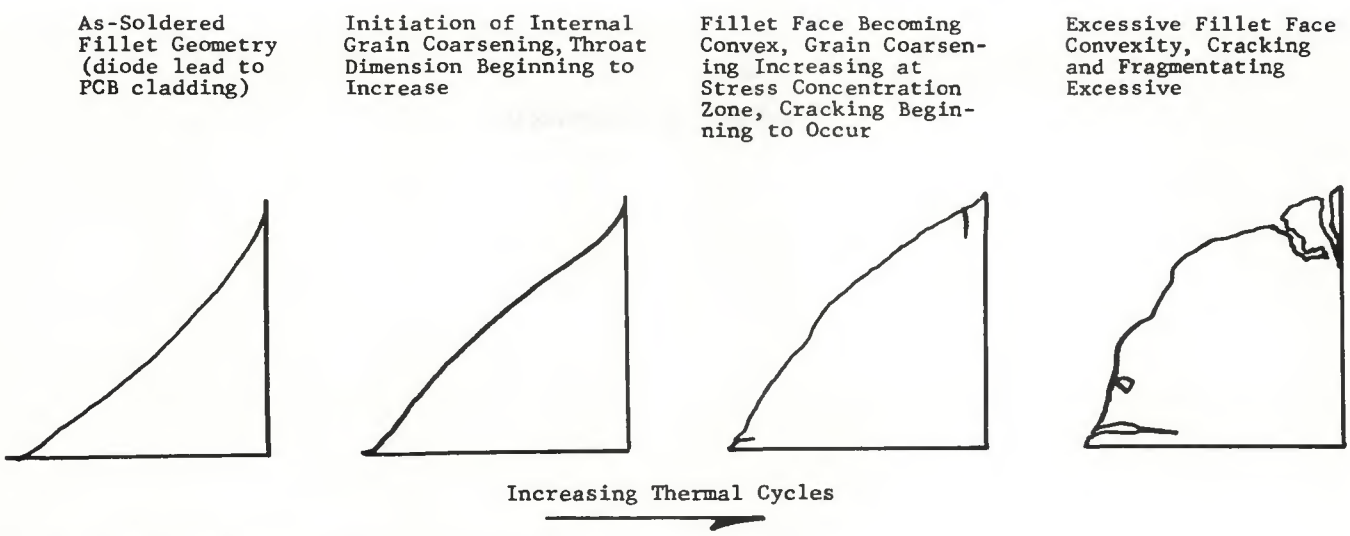

Fig. 15 — Solder fillet geometric change during thermal cycle stress failure mode

thermal cycling, a load is applied to the root area of the fillet and thus a twisting load is applied about plane C. As a result of the twisting load, fracture is starting to occur at the fillet toe and through the throat region of the fillet. Upon heatup of the joint, differences in expansion between the solder and the pin at A result in a stress which applies a shear load to the solder fillet leg. The pin expansion also applies loads to the fillet. At the same time a shear load is applied through the fillet throat at C. Due to the expansion differences between the solder and copper-polyimide board, a shear load is applied at B. These stresses produce progressive deformation as shown in Fig. 15.

The primary area of cracking is the toe region of the solder-pin interface. As depicted in the Fig. 14 model, it is in this region that multiaxial stress systems are applying shear and compressive loading to the solder/pin interface. A "hinged" twisting moment is applied to the throat region of the fillet and results in grain coarsening at the throat and leg regions of the solder fillet microstructure which produce fragments.

Therefore, one can conclude that during the application of stress to the fillet several phenomena are occurring which include the coarsening of the microstructure, deformation of the solder alloy, crack initiation at the toe regions of the fillet, alignment of lead-rich phases at the pin and copper interfaces, and depletion of tin at fillet-leg interfaces.

Conclusions

1. Low frequency thermal cycling between −65 and +150 C produced solder joint cracking with all solder alloys.

2. The eutectic solder alloy has greatest propensity for crack initiation and joint failure as measured by circuit continuity.

3. The primary mode of crack initiation in all alloys is in the solder fillet toe region adjacent to the pin.

4. With all solder alloys the toe region crack at the pin extended 360 deg.

5. Crack propagation direction in the 63Sn, 50Sn, and 40Sn alloys was adjacent to the pin/solder fillet interface.

6. Crack propagation in the 70Sn alloy was multidirectional through the throat regions of the fillet.

7. The metallurgical mechanism for cracking in the 63Sn, 50Sn, and 40Sn alloys involves failures due to stress rupture and thermal fatigue. Crack initiation is occurring in the form of intergranular separations at the fillet toe, as evidenced by fragmentation. Crack propagation is proceeding in the aligned lead-rich areas at the solder/pin interface. The crack, when confronted with tin-rich grains, propagates between the tin-rich grain and the lead-rich phase.

Fatigue of Welded Steel Structures

Prepared by W. H. Munse and Edited by LaMotte Grover

Published in 1964 by the Welding Research Council, the "fatigue" book is still a good reference on the fundamental aspects of designing welded steel structures against cyclic loading. The influence of weld defects upon fatigue strength is discussed at a number of points in this book. The question of how to evaluate such defects in general and how to avoid them and make corrections will naturally occur to some readers. Accordingly, at the suggestion of several interested parties, a discussion of weld defects, their causes and methods of correction are briefly discussed in Chapter 5.

Following this general discussion, information and data from many laboratory tests of welded structural members and connections are presented along with an analysis of these data. These laboratory studies were carried out by numerous investigators, on a variety of materials, with a multitude of different types of specimens, and using various types of testing machines. The effects of many variables have been studied.

The price of this book is $9.00. Orders should be sent with payment to the Welding Research Council, United Engineering Center, 345 East 47th Street, New York, N.Y. 10017.

WRC Bulletin
No. 195
June 1974

"A Review of Bounding Techniques in Shakedown and Ratcheting at Elevated Temperatures"
by F. A. Leckie

"A Review of Creep Instability in High-Temperature Piping and Pressure Vessels"
by J. C. Gerdeen and V. K. Sazawal

"Upper Bounds for Accumulated Strains due to Creep Ratcheting"
by W. J. O'Donnell and J. Porowski

"Cyclic Creep — An Interpretive Literature Survey"
by Erhard Krempl

In recent years considerable effort has been devoted to developing a methodology based on detailed analysis to design structures which will operate under conditions of high temperature and periodic large thermal transients such that there exists a high level of confidence in their structural integrity. This methodology encompasses analytical methods, material behavior and design criteria. There has been excellent progress in all of these areas; however, it has become obvious that simplified procedures are needed, since the costs associated with performing a rigorous time-history analysis of a structure which is subjected to significant transient loadings while operating in the creep regime are very high, particularly if three-dimensional representation is required.

The Pressure Vessel Research Committee believes that progress in further developing this methodology will be assisted by the creation and wide distribution of a series of topical reports. This report series will serve to inform both by making available techniques and data which are relatively unknown in this country and by summarizing the current state of the art. In this manner the PVRC believes that technical progress can be stimulated and focused. However, the technology is in the developmental state and a full description of ancillary information is often not available (e.g., a complete description of the creep and plasticity response of a candidate material). Also, sufficient confirmatory experimental data on structures of similar geometries, materials and operating conditions does not exist for many of the proposed design methods such as those contained in the following report. Experimental programs such as those sponsored by the USAEC are expected to provide such confirmation and define the range of applicability of proposed methods. Thus the topical reports published in *WRC Bulletin 195* are not recommendations by the PVRC to industry on the appropriate technique for pressure-vessel design at this time, but rather are topical reports of the status of an aspect of elevated temperature design at a point in time to aid the current development work in this field.

For structures other than semi-infinite right circular cylinders of uniform thickness subjected to continuous internal pressure and cyclic radial thermal gradients, no closed form analytical methods of demonstrated conservatism exist. The use of finite element time-history analysis has proven to be, on occasion, extremely expensive. Thus a clear and urgent need exists for the development of simplified analytical techniques to permit the economic evaluation of potential ratcheting configurations.

The concepts discussed in these reports are expected to have significant value in reducing the analytical efforts for the design of elevated temperature structures. At the current time insufficient experimental data are available to permit the PVRC to endorse the techniques for bounding the response of potential ratcheting problems. Further experimental data on the basic response of candidate materials as well as ratcheting experiments on typical structures are required. These reports are recommended to the industry as a source of potentially valuable techniques. It is believed that these proposals deserve detailed examination and should be tested against the body of experimental data as it becomes available.

The price of *WRC Bulletin 195* is $11.00. Orders should be sent to the Welding Research Council, United Engineering Center, 345 East 47th St., New York, N.Y. 10017.